Oil & Natural Gas Technology

DOE Award No.: DE-FE0009904
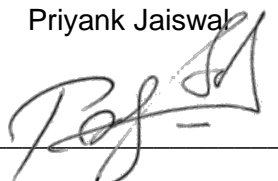
Quarterly Research Performance Progress Report (Period ending 9/31/2014)

Structural and Stratigraphic Controls on Methane Hydrate occurance and distribution: Gulf of Mexico, Walker Ridge 313 and Green Canyon 955

Project Period: 10/01/2012 – 09/30/2015

Submitted by:

Priyank Jaiswal

_____

Signature

Office of Fossil Energy

Executive Summary

This quarterly progress summarizes the progress made towards Phase 2, Subtask 3.2 – 3.4 which comprises Full Waveform Inversion of OBS data acquired by the USGS.

Background

The overall objective is to identify and understand structural and stratigraphic controls on hydrate accumulation and distribution in leased blocks WR313 (WR: Walker Ridge) and GC955 (GC: Green Canyon) in the Gulf of Mexico using seismic and well data (Figure 1). The effort is to be completed in three phases. In the first phase, the objective is to create a large-sale (resolution in the order of Fresnel zone) P-wave velocity model using traveltime inversion and a corresponding depth image using pre-stack depth migration (PSDM). This phase was completed in due time.

In the second phase, which is the topic of this report, the objective is to refine the resolution of the P-wave velocity model created in the first phase to the order of seismic wavelength using full-waveform inversion and simultaneously create P-wave velocity (V_P) and P-wave attenuation (Q_P^{-1}) model. At this stage, we have completed the second phase and report the updated velocity model and the attenuation model in this report along with the geologic interpretation of the depth image with the help of the high-resolute velocity model and attenuation model.

The third phase has two objectives. The first objective is to create a hydrate distribution map with the help of P-wave velocity and attenuation model created in the second phase and standard rock physics modeling method. The second objective is to jointly interpret the saturation map, Full-Waveform Inversion (FWI) velocity and attenuation, and the PSDM image to determine the structural and stratigraphic controls on hydrate occurrence and distribution.

Approach

Previously both OBS and MCS data, obtained from USGS, we set up for processing in ProMAX© processing software using the navigation data made available from the field (Figure 1). After setting up the navigation, the data were imported into and visually verified for their correctness. Following this, the OBS data were processed for clock drift and processed. The MCS data were also processed to ctreate a stack. The stacked data were then depth migrated and verified with the well depths. A large-sale (resolution in the order of Fresnel zone) P-wave velocity model using traveltime inversion and a corresponding depth image using pre-stack depth migration (PSDM) were generated through inversion using an approach known as Unified Imaging (UI), which was developed by Jaiswal and Zelt (2008) as a way of testing the Deragowski principle, i.e, the consistency of a velocity model with its corresponding depth migrated image. The velocity profile from traveltime inversion shows a background trends of the sonic log (Figure 2). However, the traveltime model is not adequate to show the details of velocity variations to explain the distribution of gas hydrate and free gas. This model is refined using Full Waveform Inversion (FWI).

We applied frequency-domain full waveform inversion (FWI) (Pratt, 1999) to the 7 OBS data (Fig. 1) in order to obtain a quantitative, high-resolution P-wave velocity model and the attenuation model. In this approach, the required forward simulations use a frequency-domain finite difference method. FWI

employs local gradient method for model optimization, in which the gradients are calculated using a back-propagation of misfits of the real wavefield and the modelling wavefield. Since FWI is a strongly non-linear inverse problem, the traveltime inversion model was used as an initial model. In order to use an FWI with the real data, a series of data preprocessing steps were required including deconvolution, resampling and windowing. The near offset (up to ±0.5 km) were also eliminated due to the observed amplitude saturation of early arrivals. Wavenumber filtering was applied to each successive gradient image, in order to mitigate receiver-side spatial aliasing, and also to enhance the recovery of low spatial wavernumber of the images at the early stages of the inversion process. The source wavelet was repeatedly re-estimated from data after each velocity update step using the linear optimization method (Pratt, 1999). Attenuation in the Pratt (1999) method is mainly a result of absorption. Attenuation is included in the inversion by specifying the velocity model (m) as a complex quantity ($m = m_r + im_i$), where the imaginary (m_i) and real (m_r) parts are related through the seismic quality factor Q (the reciprocal of attenuation) as
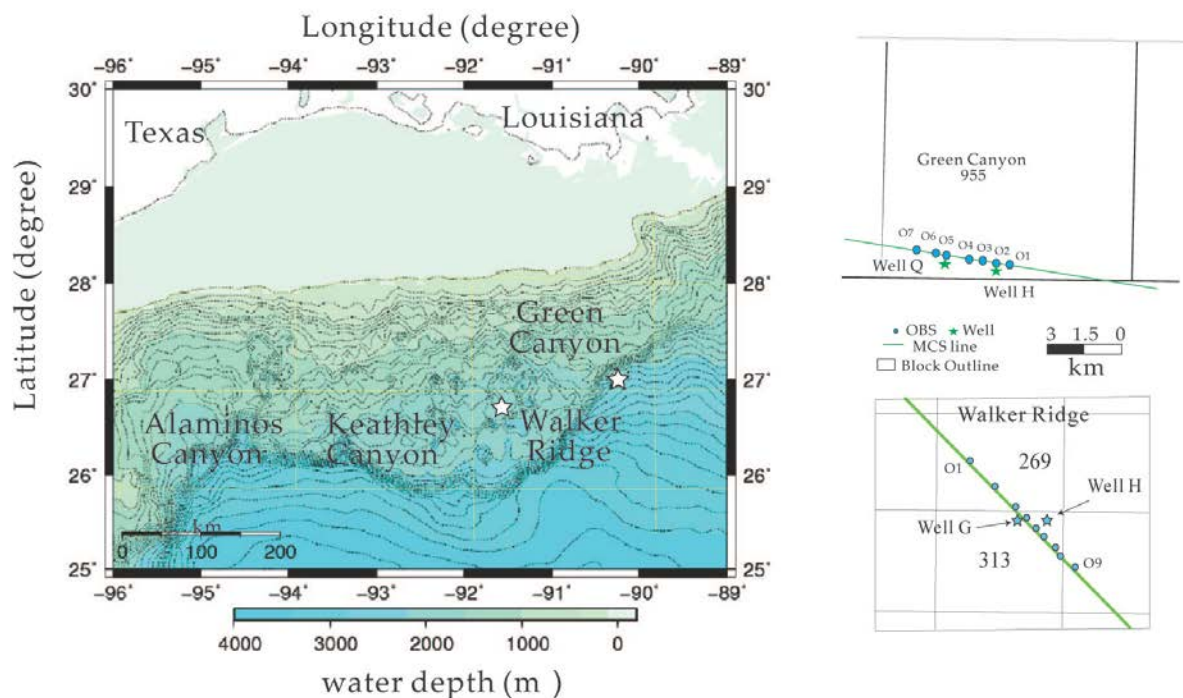
$$m_i = -\frac{m_r}{2Q}.$$

Figure 1. Base map. Seafloor bathymetry of Gulf of Mexico showing the location of the study area at the mouth of Green Canyon. The acquisition layout within the leased block 955 (GC955) is shown in the inset. Solid line is the track of the Multi-Channel Seismic (MCS) profile. Solid circles are location of Ocean Bottom Seismometers (OBSs) O1 – O7. Solid stars mark the locations of the wells Q and H that were drilling during the Joint Industry Project Leg II (JIP II).
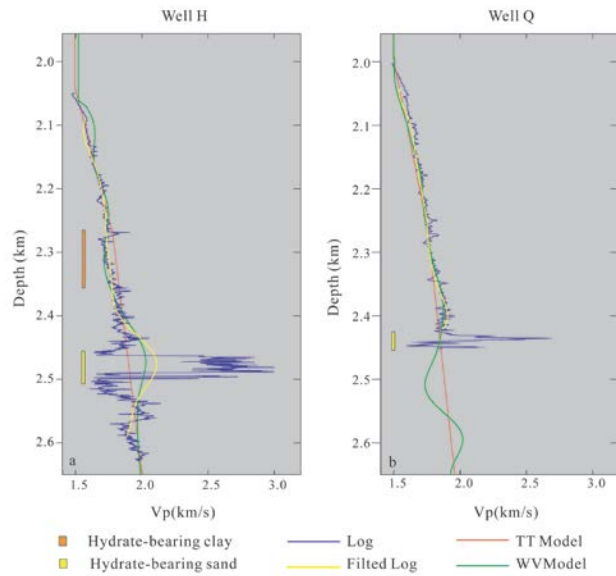
Figure 2. FWI V$_P$ comparison with sonic logs from a) Well H and (b) Well Q. In (a) and (b) the color codes are as follows: blue is the sonic log, yellow is the reconstructed log (see text for details), red is the VP from the starting model (Figure 3a), and green is the VP from the final model (Figure 3b).
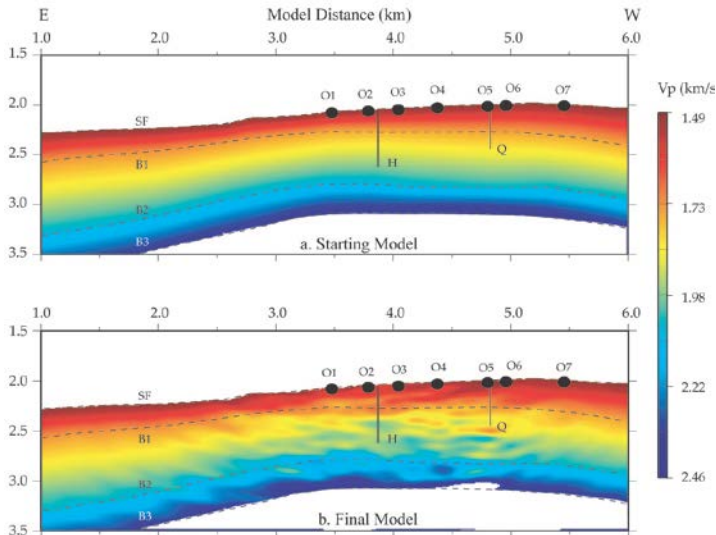

Figure 3. P-wave velocity (V$_P$) models. (a) Starting model from composite traveltime inversion – depth migration (Paper1) (b) Final model from FWI. Symbols have the following meanings. SF is the seafloor; B1 – 3 are horizons used in Paper1 to develop the starting model; O1 – 7 are OBS locations; and H and Q are the well locations.

The initial model for FWI was the final V$_P$ model developed from traveltime inversion (Figure 3a). The initial source for FWI was a minimum phase ricker wavelet. As a first step, using the traveltime model, a new source was estimated. Based on the reciprocity principle, OBSs were assumed as sources and the ship locations from where the actual shots were fired were assumed as receivers. Thus, the source inversion required only seven independent source corresponding to seven OBS gathers. The first inverted source was used for forward modeling to ensure the simulated seafloor arrivals are within half-cycle of the field seafloor arrivals. Next, keeping this source and the traveltime model stationary, the minimum frequencies in the data, 8.25, 8.5 and 8.75 Hz were simultaneously inverted resulting in very broad and smooth updates (Figure 4a). Next, with the inverted V$_P$ model, a new source was estimated and the process was repeated for groups of frequencies up to 21.75 Hz. Each group comprised 3 frequencies space 0.25Hz apart.

Essential to obtaining meaningful result from FWI was cosine tapering of the gradient at the seafloor to balance the updates in the deeper subsurface. The iterative inversion in each frequency group was halted after the reduction in the misfit function was less than 1%. The V$_P$ model became excessively

noisy after the inversion of 21.75 Hz. FWI was halted at this stage. Between the minimum and maximum frequencies, inversion of only two frequency groups, 15.25 – 15.75 Hz (Figure 4b) and 19.25 – 19.75 Hz (Figure 4c), resulted in reasonably large updates (5% or higher) in their respective models. The updates from rest of the frequencies were within 1-2%. The model from inversion of 21.25 – 21.75 Hz, although with reasonable updates (Figure 4d), did not satisfy assessment criteria set in this paper (see below). A new inversion round starting from 8.25 Hz was made used the FWI model from 15.25 – 15.75 Hz (Figure 4b) as the starting model. In the second round of inversion, the objective function could be minimized more readily and the updates resolved finer structures (Figures 4e – h). The model after 21.25 – 21.75 Hz inversion better satisfied the assessment criteria as well. A third round was also attempted, but was not successful in the inversion diverged even at lowest frequencies. The V_P model after the second round of inversion is considered final (Figure 3b).
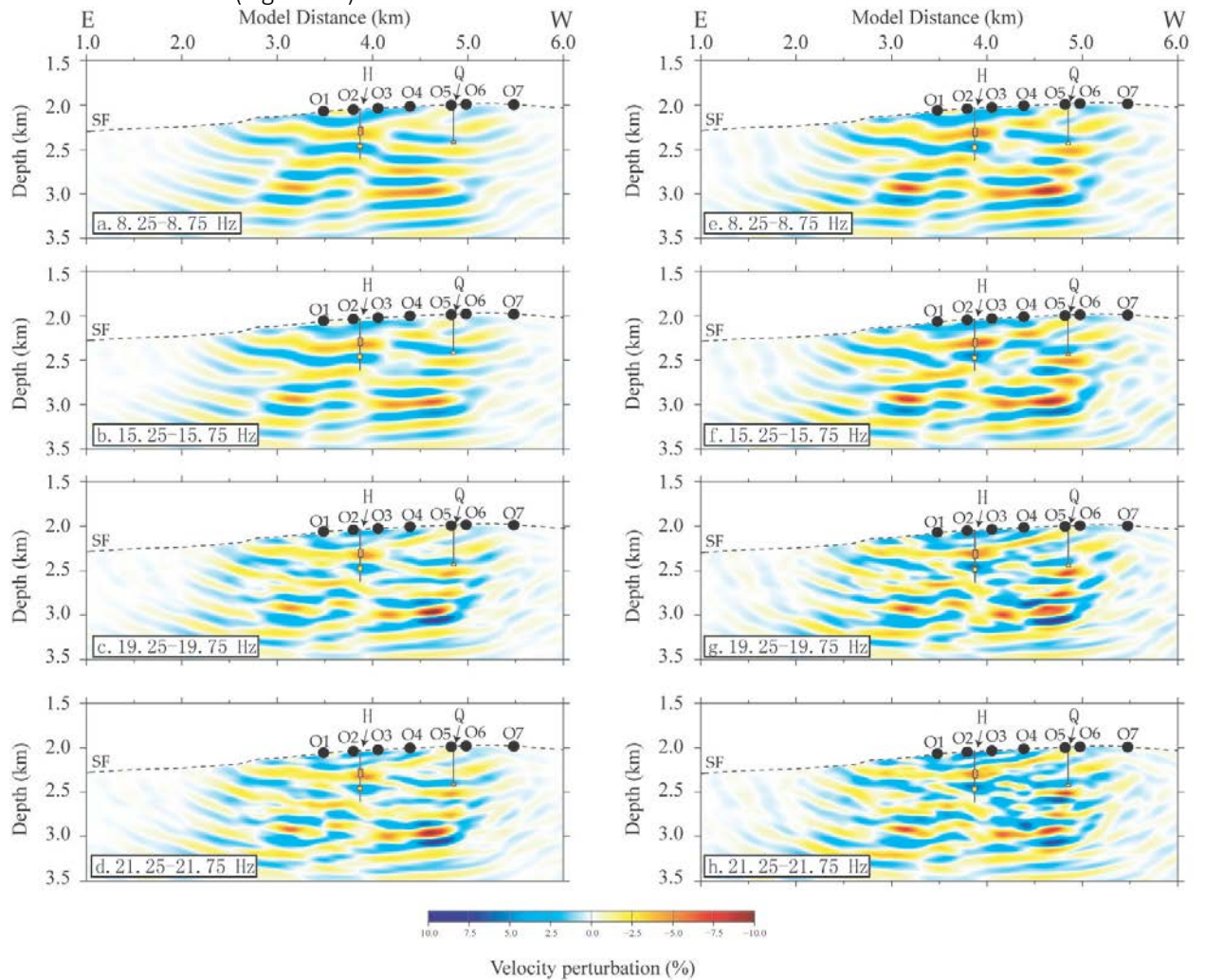

Figure 4. Velocity perturbations between the initial model and updated model. Model in (a) through (e) are from inversion of 2.25-2.75 Hz, 6.25-6.75 Hz, 9.25-9.75 Hz, 13.25-13.75 Hz, 17.25-17.75 Hz. The curves at the wells show the velocity perturbations between the initial model and the log velocity.
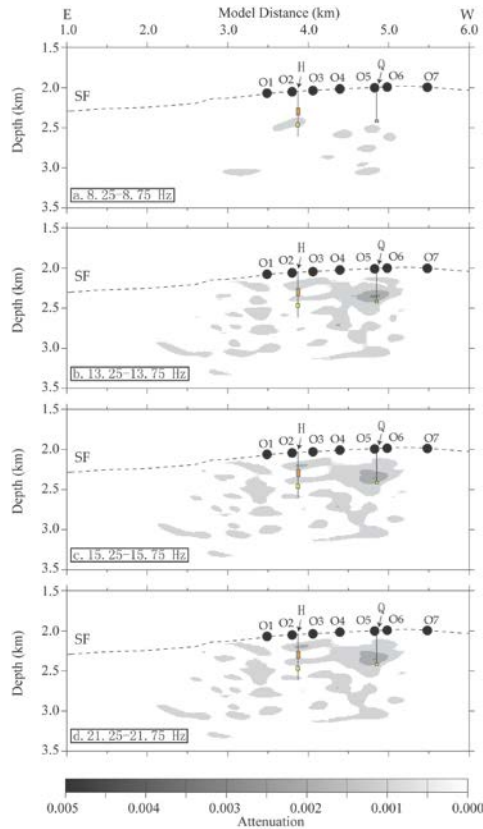
Figure 5. FWI attenuation (QP-1) updates. From inversion for a) 8.25 − 8.75 Hz; b) 15.25 − 15.75 Hz; c) 19.25 − 19.75 Hz, and d) 21.25 − 21.75 Hz using a zero starting QP-1 model and Figure 4h as the starting VP model. Symbols and colors have the same meaning as in Figure 4. The hydrate-bearing sediments appear to be non-attenuative.

The VP model from the second round and the corresponding source were used for estimating QP-1 updates. The initial QP-1 model assumed zero attenuation. Inversion of the lowest frequency group, 8.25-8.75 Hz, yields the first set of QP-1 updates which were fairly smooth in character (Figure 5a). Successive inversion of higher frequencies groups resolved the finer-scale attenuation structure (Figures 5b through d). For consistency, the frequency groups were kept same as in the VP inversion. Both the source and the VP were allowed to change simultaneously in each step of QP-1 inversion. However, the VP and source updates were minimal most likely due to the higher sensitivity of amplitudes towards QP-1 (Jaiswal et al., 2012). As like the VP inversion, frequencies over 21.75 Hz yielded very noisy models. The attenuation model from inversion of 21.25 − 21.75 Hz was considered final (Figure 5d).

Results:
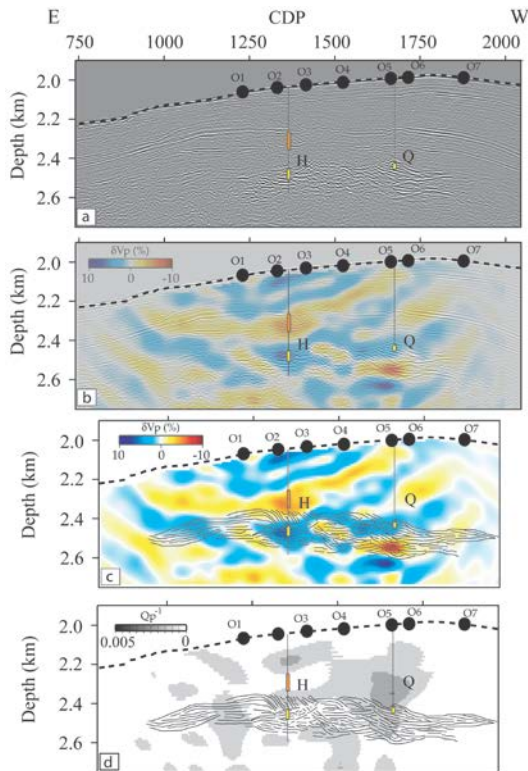
Figure 6. Composite interpretation. (a) Final depth image (from Paper1). (b) Overlay of the final depth image and final VP perturbations. Overlay of the interpreted channel system (from Paper1) on (c) the final VP perturbations and (d) the final attenuation model. Symbols and colors have the same meaning as Figure 4.

Previously, using a depth migrated profile (previous report), the hydrate-bearing sand in wells H and Q were interpreted as a part of a channel system where Well H penetrated the axis and Well Q penetrated the levee (Figure 6a). An overlay of the depth image and the final perturbation model does not show any correspondence between the V_P perturbations trends and the stratigraphy (Figure 6b). Within the channel system, the perturbations were more scattered than above or below it, which probably indicates compartmentalized but with no bearings on the internal connectivity. It is possible that the compartments referred above were merely a function of grain size and sorting.

In absence of the sonic logs, it is impossible to relate the V_P perturbations to hydrate or free gas. The sonic log in well H suggested over 20% V_P increase over the background within the hydrate-bearing sands. The seismic, however, showed only a modest increase of ~10%. It does not imply that sonic frequencies were insensitive to hydrates, but that they see an averaged effect over a larger volume of sediments than the logs. The velocity anomaly is seismic could have matched the well logs probably if the hydrate-bearing sands were spatially (both vertically and laterally) more extensive. Within the channel-levee complex, the maximum velocity increase is at the location of Well H (Figure 6c). Likewise the maximum velocity decrease is at the base of Well Q (Figure 6c), where free gas was confirmed. Away from the wells H and Q, within the resolution of seismic only a modest presence of hydrate or free gas can be speculated. Away from the wells, the positive and negative perturbations within the channel complex could also be indicative of lithological changes rather than hydrate and free gas variation.

  An overlay of the channel interpretation on the attenuation model show that the two known hydrate-bearing zones sampled along Well H, have subdued attenuation compared to the background sediment. Attenuation is most significant in the vicinity of well Q. It is noteable that attenuation is not as high below the Well Q where free gas was confirmed, as it is along the wellbore immediately above the gas pocket. White (1975) argued that attenuation and gas saturation may not have a linear relation; attenuation initially increases with increasing gas saturation but then beyond a certain saturation threshold, decreased as saturation increases. The attenuation structure near Well Q raises the possibility of presence of free gas (probably in the bubble phase) within the upper 400m of the stratigraphy from the seafloor. As amplitudes are more sensitive to fluid content than velocities, the gas must be in low enough saturation to not affect the V_P but manifest in the attenuation model.

Conclusions:

At the end of this phase of work, our conclusions are as follows. FWI yielded reliable estimates even with a visco-acoustic approximation to an elastic dataset. Success of FWI strongly depends on data preconditioning and the starting model. The minimum and the maximum usable inversion frequencies were 8.25 and 21.75 Hz respectively. In between, frequencies spaced 0.25Hz apart were inverted in groups of 3. A multi-scale FWI approach prevents cycle-skipping. The V_P estimation was done in two rounds. In the first round the traveltime inversion model was using as the starting model. In the second round, the model from inversion of 15Hz group was used as the starting model. Criteria used to halt the FWI included the reliability of evolving V_P and Q_P^{-1} perturbations, similarity of the real and simulated data, and the convergence of the objective function. A composite reflectivity and V_P interpretation suggests that the sand-dominated channel system is internally compartmentalized. Both hydrate and free gas have a patchy distribution and hydrated sediments appear to be non-attenuative.

References:

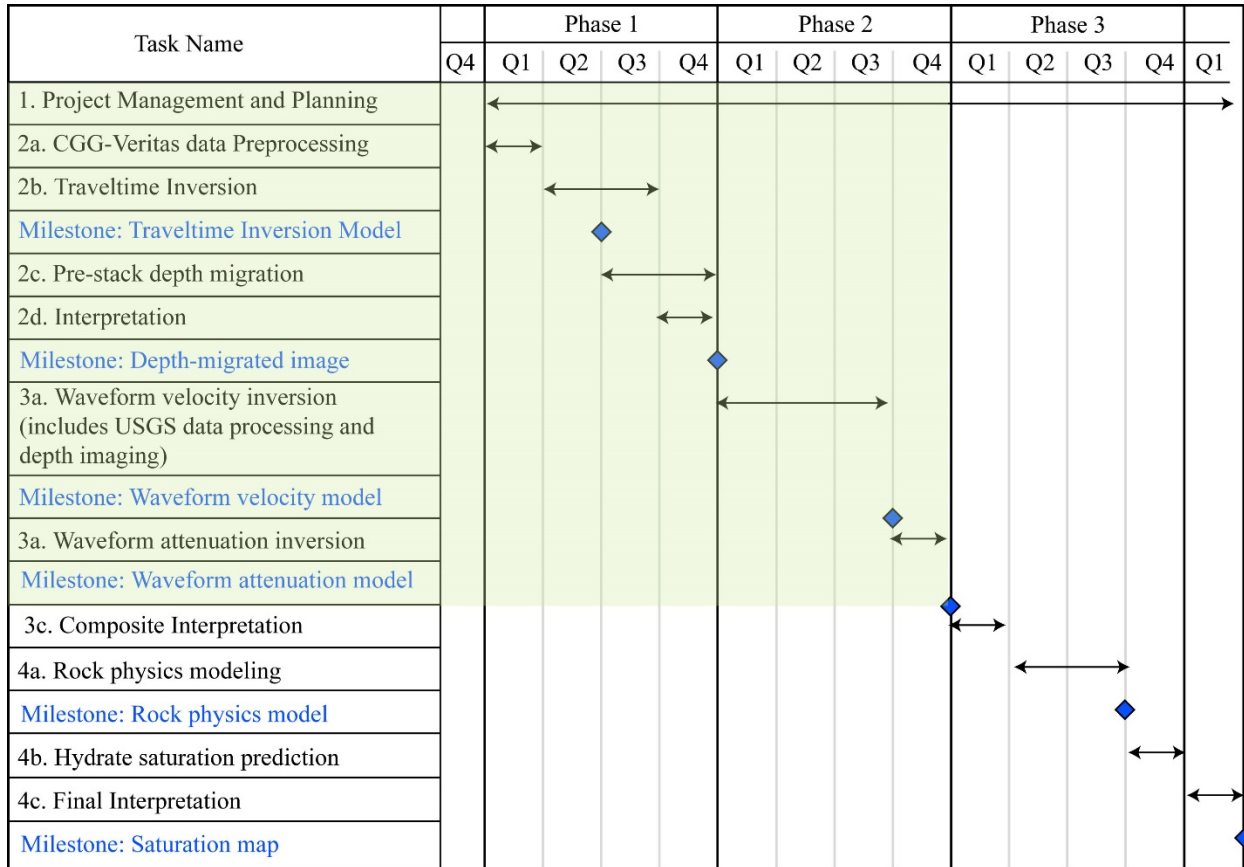Jaiswal, P., and C. A. Zelt. 2008, Unified imaging of multichannel seismic data: Combining traveltime inversion and prestack depth migration. Geophysics, 73, no. 5, VE269-VE280. doi: 10.1190/1.2957761.

Jaiswal P., P. Dewangan, T. Ramprasad, C.A. Zelt, 2012. Seismic characterization of hydrates in faulted, fine-grained sediments of Krishna-Godavari Basin: Full Waveform Inversion: Journal of Geophysical

Research – Solid Earth, 117, B10305.Pratt, R.G., 1999. Seismic waveform inversion in the frequency domain, Part 1: Theory, and verification in a physical scale model. Geophysics, 64, 888-901.

White, J. 1975, Computed seismic speeds and attenuation in rocks with partial gas saturation. Geophysics, 40, no. 2,224-232. doi: doi:10.1190/1.1440520.

Project milestone chart

Task Name	Q4	Phase 1				Phase 2				Phase 3				Q1
		Q1	Q2	Q3	Q4	Q1	Q2	Q3	Q4	Q1	Q2	Q3	Q4	
1. Project Management and Planning		←												→
2a. CGG-Veritas data Preprocessing		←→												
2b. Traveltime Inversion			←→											
Milestone: Traveltime Inversion Model			◆											
2c. Pre-stack depth migration				←→										
2d. Interpretation					←→									
Milestone: Depth-migrated image					◆									
3a. Waveform velocity inversion (includes USGS data processing and depth imaging)						←——→								
Milestone: Waveform velocity model								◆						
3a. Waveform attenuation inversion								←→						
Milestone: Waveform attenuation model														
3c. Composite Interpretation									◆←→					
4a. Rock physics modeling										←→				
Milestone: Rock physics model												◆		
4b. Hydrate saturation prediction												←→		
4c. Final Interpretation													←→	
Milestone: Saturation map														◆

The project is on target till date. Tasks already completed in the milestone chart are shaded in green.

Milestone Status:

Milestone	Description	Status	Schedule
Traveltime Inversion Model	The recipient shall compare the real and predicted reflection traveltimes from the final velocity model to be used for PSDM.	Done for CGGVeritas Datase and for the USGS dataset	Completed on target
Depth Migrated Image	The recipient shall compare structure and stratigraphy between the final depth image and images in literature and SSRs.	Done	Completed on target
Waveform velocity model	The recipient shall compare waveform inversion velocity and sonic logs at well locations.	Done	Completed On target
Waveform attenuation model	The recipient shall compare real and synthetic simulated data.	Done	Completed On target
Rock physics model	The recipient shall compare predicted hydrate saturation at well locations with that available in the literature and methods of other DOE funded PIs, if available.	Ongoing	On target
Saturation map	The recipient shall compare consistency between hydrate distribution and structural/stratigraphic features interpreted in the study area.	Ongoing	On target

National Energy Technology Laboratory

626 Cochrans Mill Road

P.O. Box 10940

Pittsburgh, PA 15236-0940

3610 Collins Ferry Road

P.O. Box 880

Morgantown, WV 26507-0880

13131 Dairy Ashford Road, Suite 225

Sugar Land, TX 77478

1450 Queen Avenue SW
Albany, OR 97321-2198

Arctic Energy Office

420 L Street, Suite 305

Anchorage, AK 99501

Visit the NETL website at:

www.netl.doe.gov

Customer Service Line: 1-800-553-7681